Anusandhanvallari
Vol 2023, No.1
June 2023
ISSN 2229-3388

Bending Characteristics of Pretwisted Composite Delaminated Stiffened Shell-A Finite Element Approach

Mrutyunjay Rout[1] and Chitaranjan Dash[2]

[1]Department of Mechanical Engineering , Government College of Engineering, Kalahandi, Bhawanipatna-766 003, India
[2]Department of Mathematics, Government College of Engineering, Kalahandi, Bhawanipatna-766 003, India
Corresponding author:
Mrutyunjay Rout
Mechanical Engineering Department, Government College of Engineering, Kalahandi, Bhawanipatna-766 002, India
E-mail: kulu2670371@yahoo.co.in

Abstract

The paper presents the bending characteristics of twisted composite stiffened cylindrical shell employing finite element method considering delamination at different locations. An eight noded isoparametric shell element based on first-order shear deformation theory is combined with a three noded isoparametric curve beam element to model the shell and the stiffener, respectively. The formulation employs a constraint technique to compute the stiffness and the mass of the stiffener, wherein the stiffness of the stiffener at the nodes are transferred to the corresponding nodes of the shell element taking into account both the curvature and eccentricity of the stiffener. Delamination at the desired location of the shell is modeled using Multipoint constraint algorithm, wherein the compatibility of resultant forces, moments and deformation are established at the delamination crack front. The influence of different parameters like delamination size and location, twist angles, the thickness of stiffener and eccentricity of stiffener under the action of mechanical loading on the static behavior of the stiffened shell are presented.

Keywords: Bending, Stiffener, Delamination, Stress, Pretwist, Composite

Nomenclature:

L, b	length and width of shell, respectively
h	Thickness of shell
n_x, n_y	number of stiffeners in x- and y- direction, respectivley
b_{st}, d_{st}	width and depth of stiffener, respectively
θ	fibre orientation
Φ	twist angle of the cylindrical shell
d	distance of centre of delamination from fixed end
a	length of delamination along the span of shell
h'	distance of delamination across the thickness from top ply
p	intensity of uniformly distributed load
$\overline{w}$	non-dimensional transverse deflection[$=10^3 wE_2h^3/(pL^4)$]

$\overline{M}_i$ non-dimensional moment resultants[$=10^3 M_i / pL^2 \quad i = x, y$]

$\overline{M}_{xy}$ non-dimensional torsion resultant[$= 10^3 M_{xy} / pL^2$]

$\overline{N}_i$ non-dimensional in-plane force resultants[$10^3 N_i / pL \quad i = x, y$]

$\overline{N}_{xy}$ non-dimensional in-plane shear resultant[$= 10^3 N_{xy} / pL$]

1. Introduction

The advantage of using composite materials over the convectional material are mainly found in aerospace, naval, automobile industries and other civil engineering application owing to its high specific strength and stiffness. The pretwisted cantilever composite cylindrical shells can be idealized as turbomachinery blades and to improve the strength to weight ratio in a cost effective manner the blades are very often integrated by stiffeners. The complexity of the stiffened structure enables most of the researchers to use numerical methods as an alternative tool to analyze its performance. There are several publications available in the open literature dealing with the static behavior of the isotropic and composite stiffened structure but some of the important works are discussed here.

Rossow and Ibrahimkhail [1] presented constraint method of finite element analysis to study the static performance of both eccentric and concentric stiffened isotropic plates while Venkatesh and Rao [2] reported the finite element analysis of eccentrically stiffened laminated cantilever cylindrical shell, wherein the shell and beam elements have 48 and 16 degrees of freedom, respectively. Later on, the same author [3] investigated the moments and strains of the eccentrically stiffened shell wherein they presented the results of the laminated hyperboloid and cylindrical stiffened shells. Liao and Reddy[4] developed a nonlinear displacement finite element model based on a principle of virtual displacement wherein a degenerated shell element in conjunction with a degenerated curved beam element used to study the nonlinear analysis of laminated, anisotropic, stiffened shells. Chattopadhyay et al.[5] reported the results of deflection and moments of simply supported blade-stiffened composite plates under transverse load employing finite element method. Goswami and Mukhopadhyay[6] studied the bending characteristics of composite concentric and eccentrically stiffened shell employing finite element method wherein a modified approach was presented to formulate curved shear flexible shell element. Mukherjee and Menghani [7] developed a higher order theory to investigate the displacement and stresses at different nodes of the laminated stiffened plates. Sinha and Mukhopadhyay [8] reported the review of static and dynamic analysis of the stiffened shells. Kolli and Chandrashekhara [9] studied the bending behavior of eccentrically stiffened composite plates under transverse loading employing finite element method considering various boundary conditions. Sadek and Tawfik [10] presented a refined model based on higher order shear deformation theory, wherein the use of shear correction coefficient was eliminated and compared the deflection and in-plane stress results of both isotropic and composite stiffened plates with available exact and numerical solutions. Prusty [11] reported a parametric study of the linear static behavior of composite hat/rectangular/T-shaped stiffened shell employing finite element method with a concept of equal displacement at the junction of shell and stiffener. Li and Xiaohui [12] proposed a higher-order global–local theory to study the bending of thick stiffened laminated plates wherein the stiffeners were considered as the laminated plates with thickness discontinuity. Das and Chakravorty [13] studied both static deflections and force/moment resultants of eccentrically stiffened composite conoidal shell subjected to concentrated load under various boundary conditions. Bhaskar and Pydah [14] developed an analytical elastic solution of blade stiffened plates wherein the plate and stiffener were considered as 3D and 2D models, respectively.

Delamination in composite structures causes a substantial loss in load carrying capacity and affects greatly to the safety of operation. Delamination occurrence in the structures is too difficult to predict, thus to

ensure the safe and efficient use of composite structure it is very essential to have a profound knowledge of the stiffened structures with delamination. Shen and Grady [15], Krawczuk et al.[16], Karmakar and Kishimoto [17] are some notable researchers to study the effect of delamination on vibration characteristics of composite beams, plates and shells, respectively while Bandyopadhyay and Karmakar [18] reported the bending characteristics of rotating pretwisted composite conical shell with delamination under hygrothermal loading.

The revolutionary work of composite plates with pretwist was performed by Qatu and Leissa [19] wherein they studied the natural frequencies and mode shapes of composite plates at various twist angles using Ritz methods. Thereafter, Kuang and Hsu [20], Lee and Yeom [21], Kee and Kim [22] and Karmakar and Kishimoto [17] extended the work of pretwisted shells while Thirupathi et al.[23] studied the static analysis of pretwisted piezoelectric actuated blades for turbomachinery applications using finite element method.

After a meticulous survey of the literature and to the best of the authors' knowledge, almost all the articles deals with either composite stiffened shells/plates without pretwist and delamination or delaminated pretwisted shell without stiffener. The static behavior of stiffened shell with pretwist and delamination has not been given attention by any of the researchers till date, thus the authors aimed to investigate the bending characteristics of the pretwisted stiffened cylindrical shell with delamination subjected transverse load. The present study is aspired to find out the deflections, in-plane stresses, force and moment resultants with the variation of size and position of delamination, twist angles, the number of stiffeners and eccentricity of stiffeners.

2. Theoretical formulation

The coordinate system of a typical laminated composite stiffened cylindrical shell with pretwist is illustrated in Figure-1, wherein the stiffener is placed parallel to *x*-direction. The finite element formulation for both shell and stiffener are as follows.

An eight-noded quadratic isoparametric element having five degrees of freedom u, v, w, α and β at each node is used in the present formulation to model the shell element. The element shape function derived from the interpolation polynomial are expressed as:

$$\begin{aligned} N_i &= (1+\xi\xi_i)(1+\eta\eta_i)(\xi\xi_i+\eta\eta_i-1)/4 && \text{(for } i=1,2,3,4\text{)} \\ N_i &= (1+\xi\xi_i)(1-\eta^2)/2 && \text{(for } i=5,7\text{)} \\ N_i &= (1+\eta\eta_i)(1-\xi^2)/2 && \text{(for } i=6,8\text{)} \end{aligned} \quad (1)$$

The displacement at any point within the element are interpolated from nodal values as:

$$u=\sum_{i=1}^{8}N_iu_i\,,\quad v=\sum_{i=1}^{8}N_iv_i\,,\quad w=\sum_{i=1}^{8}N_iw_i\,,\quad \alpha=\sum_{i=1}^{8}N_i\alpha_i \text{ and } \beta=\sum_{i=1}^{8}N_i\beta_i \quad (2)$$

The generalized strains composed of mid-plane strains and curvatures are expressed as

$$\{\varepsilon_x\ \varepsilon_y\ \gamma_{xy}\ \gamma_{xz}\ \gamma_{yz}\}^T=\{\varepsilon_x^0\ \varepsilon_y^0\ \gamma_{xy}^0\ \gamma_{xz}^0\ \gamma_{yz}^0\}^T+z\{\kappa_x\ \kappa_y\ \kappa_{xy}\ \kappa_{xz}\ \kappa_{yz}\}^T \quad (3)$$

where

$$\begin{bmatrix} \varepsilon_x^0 \\ \varepsilon_y^0 \\ \gamma_{xy}^0 \\ \gamma_{xz}^0 \\ \gamma_{yz}^0 \end{bmatrix} = \begin{bmatrix} \frac{\partial u}{\partial x} & \frac{\partial v}{\partial y} + \frac{w}{R_y} & \frac{\partial u}{\partial y} + \frac{\partial v}{\partial x} + \frac{2w}{R_{xy}} & \alpha + \frac{\partial w}{\partial x} & \beta + \frac{\partial w}{\partial y} \end{bmatrix}^T \text{ and}$$

$$\begin{bmatrix} \kappa_x \\ \kappa_y \\ \kappa_{xy} \\ \kappa_{xz} \\ \kappa_{yz} \end{bmatrix} = \begin{bmatrix} \frac{\partial \alpha}{\partial x} & \frac{\partial \beta}{\partial y} & \frac{\partial \alpha}{\partial y} + \frac{\partial \beta}{\partial x} & 0 & 0 \end{bmatrix}^T$$

The relation of strain and displacement of the shell element is expressed as

$$\{\varepsilon\} = [B]\{d_e\} \tag{4}$$

where $\{d_e\} = [u_1 \quad v_1 \quad w_1 \quad \alpha_1 \quad \beta_1 \cdots\cdots\cdots u_8 \quad v_8 \quad w_8 \quad \alpha_8 \quad \beta_8]^T$

$$[B] = \sum_{i=1}^{8} \begin{bmatrix} N_{i,x} & 0 & 0 & 0 & 0 \\ 0 & N_{i,y} & N_i / R_y & 0 & 0 \\ N_{i,y} & N_{i,x} & 2N_i / R_{xy} & 0 & 0 \\ 0 & 0 & 0 & N_{i,x} & 0 \\ 0 & 0 & 0 & 0 & N_{i,y} \\ 0 & 0 & 0 & N_{i,y} & N_{i,x} \\ 0 & 0 & N_{i,x} & N_i & 0 \\ 0 & 0 & N_{i,y} & 0 & N_i \end{bmatrix} \tag{5}$$

$[B]$ is the strain displacement matrix and $\{d_e\}$ is the nodal displacement vector.
The Stresses at a point in the laminate are expressed as

$$\begin{Bmatrix} \sigma_x \\ \sigma_y \\ \tau_{xy} \\ \tau_{xz} \\ \tau_{yz} \end{Bmatrix} = \begin{bmatrix} \overline{Q}_{11} & \overline{Q}_{12} & \overline{Q}_{16} & 0 & 0 \\ \overline{Q}_{21} & \overline{Q}_{22} & \overline{Q}_{26} & 0 & 0 \\ \overline{Q}_{16} & \overline{Q}_{26} & \overline{Q}_{66} & 0 & 0 \\ 0 & 0 & 0 & \overline{Q}_{44} & \overline{Q}_{45} \\ 0 & 0 & 0 & \overline{Q}_{45} & \overline{Q}_{55} \end{bmatrix} \begin{Bmatrix} \varepsilon_x \\ \varepsilon_y \\ \gamma_{xy} \\ \gamma_{xz} \\ \gamma_{yz} \end{Bmatrix} \tag{6}$$

The constitutive equation for the composite shell is given by

$$\{F\} = [D]\{\varepsilon\} \tag{7}$$

where $\{F\} = [N_x \; N_y \; N_{xy} \; M_x \; M_y \; M_{xy} \; Q_{xz} \; Q_{yz}]^T$

N_x, N_y and N_{xy} are the in-plane force resultants; M_x, M_y and M_{xy} are the moment resultants; Q_{xz} and Q_{yz} are the transverse shear resultants.

The elasticity matrix of the composite laminate is defined as

$$[D] = \begin{bmatrix} A_{ij} & B_{ij} & 0 \\ B_{ij} & D_{ij} & 0 \\ 0 & 0 & S_{ij} \end{bmatrix} \tag{8}$$

$$(A_{ij}, B_{ij}, D_{ij}) = \sum_{k=1}^{nl} \int_{z_{k-1}}^{z_k} ([\overline{Q}_{ij}])_k (1, z, z^2)\, dz, \quad i, j = 1, 2, 6$$

$$(S_{ij}) = k_s \sum_{k=1}^{nl} \int_{z_{k-1}}^{z_k} ([\overline{Q}_{ij}])_k\, dz, \quad i, j = 4,5$$

where $[\overline{Q}_{ij}]$ is the off-axis elastic constant matrix, k_s is the shear correction factor to account for parabolic variation of the transverse shear strains and is approximately taken as 5/6 and nl is the number of layers.

The element stiffness matrix of the shell is expressed

$$[K_{she}] = \int_{-1}^{1} \int_{-1}^{1} [B]^T [D][B] |J| d\xi d\eta \tag{9}$$

where $[B]$ is the strain-displacement matrix and $|J|$ is the determinant of Jacobian matrix.

The numerical integration of the equation (9) is performed by using Gaussian quadrature with 2×2 reduced integration to avoid shear locking.

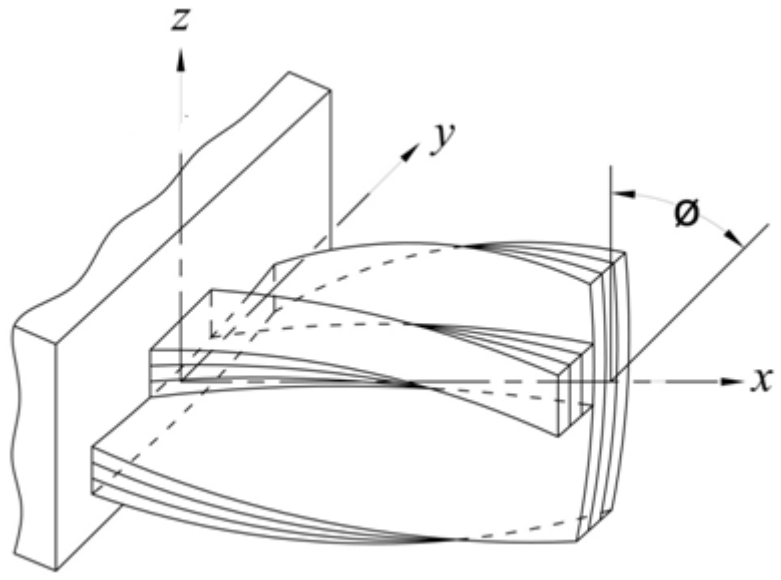

Figure 1. Coordinate system of a laminated composite cylindrical stiffened shell with pretwist.

Beam element of rectangular section of uniform cross-section($b_{st} \times d_{st}$) are considered for modeling the stiffeners. The isoparametric curved three-node beam elements with four degrees of freedom(two translation and two rotation) per node are chosen for modeling the stiffeners. The shape functions of the x- and y- stiffeners are expressed as follows:

For x-directional stiffeners,

$$\begin{aligned} N_i^{sx} &= 0.5\xi\xi_i(1+\xi\xi_i) && \text{for } i=1,3 \\ N_i^{sx} &= (1-\xi^2) && \text{for } i=2 \end{aligned} \tag{10}$$

For y-directional stiffeners,

$$\begin{aligned} N_i^{sy} &= 0.5\eta\eta_i(1+\eta\eta_i) && \text{for } i=1,3 \\ N_i^{sy} &= (1-\eta^2) && \text{for } i=2 \end{aligned} \tag{11}$$

The generalized displacements of x-/y-directional stiffener element can be interpolated from the nodal values as follows:

For the x-directional stiffeners,

$$u_{sx} = \sum_{i=1}^{3} N_i^{sx} u_{sxi}\ ,\ w_{sx} = \sum_{i=1}^{3} N_i^{sx} w_{sxi}\ ,\alpha_{sx} = \sum_{i=1}^{3} N_i^{sx} \alpha_{sxi} \text{ and } \beta_{sx} = \sum_{i=1}^{3} N_i^{sx} \beta_{sxi} \tag{12}$$

For the y-directional stiffeners,

$$v_{sy} = \sum_{i=1}^{3} N_i^{sy} v_{syi}\ ,\ w_{sy} = \sum_{i=1}^{3} N_i^{sy} w_{syi}\ ,\alpha_{sy} = \sum_{i=1}^{3} N_i^{sy} \alpha_{syi} \text{ and } \beta_{sy} = \sum_{i=1}^{3} N_i^{sy} \beta_{syi} \tag{13}$$

The generalized displacement vector of a x-and y-stiffener element is expressed in terms of the shape functions and nodal degrees of freedom as

$$\begin{aligned} \{\delta_{sx}\} &= [N^{sx}]\{\delta_{sxi}\} \\ \{\delta_{sy}\} &= [N^{sy}]\{\delta_{syi}\} \end{aligned} \tag{14}$$

The stress resultants for the x- and y-directional stiffness are

$$\begin{aligned} [F_{sx}] &= [E_{sx}]\{\varepsilon_{sx}\} = [E_{sx}][B_{sx}]\{\delta_{sxi}\} \\ [F_{sy}] &= [E_{sy}]\{\varepsilon_{sy}\} = [E_{sy}][B_{sy}]\{\delta_{syi}\} \end{aligned} \tag{15}$$

where

$$\{F_{sx}\} = \{N_x^{sx}\ M_x^{sx}\ T_x^{sx}\ Q_x^{sx}\}^T$$

$$\{F_{sy}\} = \{N_y^{sy}\ M_y^{sy}\ T_y^{sy}\ Q_y^{sy}\}^T$$

$$\{\varepsilon_{sx}\} = \{u_{sx,x}\quad \alpha_{sx,x}\quad \beta_{sx,x}\quad (\alpha_{sx} + w_{sx,x})\}^T$$

$$\{\varepsilon_{sy}\} = \{(v_{sy,y} + \frac{w_{sy}}{R_y})\quad \beta_{sy,y}\quad \alpha_{sy,y}\quad (\beta_{sy} + w_{sy,y})\}^T$$

$$\{\delta_{sx}\} = \{u_{sx}\ w_{sx}\ \alpha_{sx}\ \beta_{sx}\}^T$$

$$\{\delta_{sy}\} = \{v_{sy}\ w_{sy}\ \alpha_{sy}\ \beta_{sy}\}^T$$

The elasticity matrices of x- and y-stiffener element are as follows:

$$[E_{sx}]=\begin{bmatrix} A_{11}^{sx}b_{st} & B_{11}^{sx}b_{st} & B_{16}^{sx}b_{st} & 0 \\ B_{11}^{sx}b_{st} & D_{11}^{sx}b_{st} & D_{16}^{sx}b_{st} & 0 \\ B_{16}^{sx}b_{st} & D_{16}^{sx}b_{st} & \frac{1}{6}(Q_{66}^{sx}+Q_{44}^{sx})d_{st}b_{st}^{3} & 0 \\ 0 & 0 & 0 & S_{44}^{sx}b_{st} \end{bmatrix} \tag{16}$$

where

$$A_{ij}^{sx}=\sum_{k=1}^{nl}(Q_{ij})_k(z_k-z_{k-1});\quad i,j=1$$

$$B_{ij}^{sx}=\frac{1}{2}\sum_{k=1}^{nl}(Q_{ij})_k(z_k^2-z_{k-1}^2);\quad i,j=1,6$$

$$D_{ij}^{sx}=\frac{1}{3}\sum_{k=1}^{nl}(Q_{ij})_k(z_k^3-z_{k-1}^3);\quad i,j=1,6$$

$$S_{ij}^{sx}=k_s\sum_{k=1}^{nl}(Q_{ij})_k(z_k-z_{k-1});\quad i,j=4$$

$$[E_{sy}]=\begin{bmatrix} A_{22}^{sy}b_{st} & B_{22}^{sy}b_{st} & B_{26}^{sy}b_{st} & 0 \\ B_{22}^{sy}b_{st} & D_{22}^{sy}b_{st} & D_{26}^{sy}b_{st} & 0 \\ B_{26}^{sy}b_{st} & D_{26}^{sy}b_{st} & \frac{1}{6}(Q_{66}^{sy}+Q_{55}^{sy})d_{st}b_{st}^{3} & 0 \\ 0 & 0 & 0 & S_{55}^{sy}b_{st} \end{bmatrix} \tag{17}$$

The element stiffness matrix of the stiffeners are
for x-directional stiffener:

$$[K_{sxe}]=\int_{-1}^{1}[B_{sx}]^T[E_{sx}][B_{sx}]\left|J^{sx}\right|d\xi \tag{18}$$

for y-directional stiffener:

$$[K_{sye}]=\int_{-1}^{1}[B_{sy}]^T[E_{sy}][B_{sy}]\left|J^{sy}\right|d\eta \tag{19}$$

Since the x-directional stiffeners are arranged along the span of the cylindrical shell, only the effects of eccentricity ($e_{sy}=(h+d_{st})/2$) will be taken into consideration to ensure the compatibility between the shell and beam element wherein the nodal degrees of freedom of the stiffener are to be transformed to the shell degrees of freedom. However, in case of y- stiffeners both the effect of curvature and eccentricity are taken into consideration and is given below:

$$u_{syi}=u_i,\ v_{syi}=\left(1+\frac{e_{sy}}{R_y}\right)v_i,\ w_{syi}=w_i,\ \alpha_{syi}=\alpha_i,\ \beta_{syi}=\beta_i \tag{20}$$

where

Based on the above equation the transformation matrix of the y-stiffener considering the effects of curvature can be written as

$$[T_C]=\begin{bmatrix}1 & 0 & 0 & 0 & 0\\ 0 & \left(1+\frac{e_{sy}}{R_y}\right) & 0 & 0 & 0\\ 0 & 0 & 1 & 0 & 0\\ 0 & 0 & 0 & 1 & 0\\ 0 & 0 & 0 & 0 & 1\end{bmatrix} \tag{21}$$

The transformation matrix of the x-/y-stiffener considering the effects of eccentricity are
for x-directional stiffener:

$$[T_e]=\begin{bmatrix}1 & 0 & 0 & e_{sx} & 0\\ 0 & 0 & 1 & 0 & 0\\ 0 & 0 & 0 & 1 & 0\\ 0 & 0 & 0 & 0 & 1\end{bmatrix} \tag{22}$$

for y-directional stiffener:

$$[T_e]=\begin{bmatrix}0 & 1 & 0 & 0 & e_{sy}\\ 0 & 0 & 1 & 0 & 0\\ 0 & 0 & 0 & 1 & 0\\ 0 & 0 & 0 & 0 & 1\end{bmatrix} \tag{23}$$

The element stiffness matrix of the stiffened shell element is obtained by adding those of the shell , x-directional stiffener and y-directional stiffener elements as follows:

$$[K_e]=[K_{she}]+[K_{sxe}]+[K_{sye}] \tag{24}$$

In general, the middle surface of a shallow shell is characterized as[18]

$$z=-\frac{1}{2}\left\{\frac{x^2}{R_x}+2\frac{xy}{R_{xy}}+\frac{y^2}{R_y}\right\} \tag{25}$$

For cylindrical shell, there is no curvature along the spanwise direction $(R_x=\infty)$. The twist angle of the shell is defined in terms of length(L) and curvature of twist (R_{xy}) as

$$\tan\phi=-\frac{L}{R_{xy}} \tag{26}$$

Multipoint constraints algorithm for delamination

The cross-sectional view of delamination crack front of a plate element is shown in Figure-2. The undelaminated region is modeled as element 1, whereas the delaminated region as element 2 and 3. The dynamic contacts between the delaminated layers have not taken into account in this formulation.

Anusandhanvallari
Vol 2023, No.1
June 2023
ISSN 2229-3388

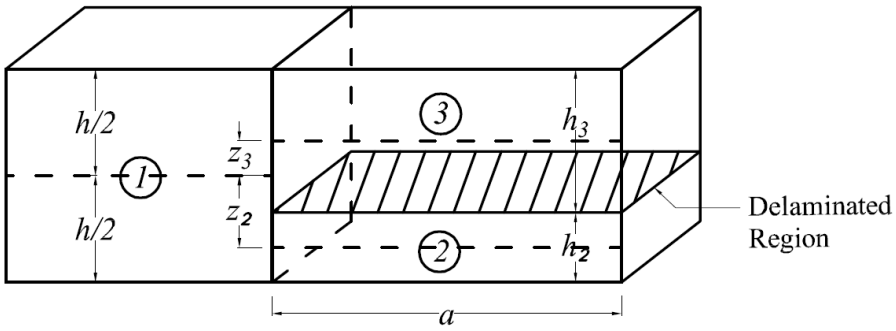

Figure 2. Plate elements at a delamination crack tip

The nodal displacement of element 2 and 3 at the crack tip are expressed as [24]:

$$\begin{aligned} u_i &= u_i' - (z - z_i)\alpha_i \\ v_i &= v_i' - (z - z_i)\beta_i \\ w_i &= w_i' \end{aligned} \tag{27}$$

where u_i', v_i', w_i' are the mid-plane displacements and z_i is the z coordinates of the mid-plane of element i. As per the constraint conditions, the transverse displacements and rotations of all the three elements must have the same values at common node and are expressed as:

$$\begin{aligned} w_1 &= w_2 = w_3 = w \\ \alpha_1 &= \alpha_2 = \alpha_3 = \alpha \\ \beta_1 &= \beta_2 = \beta_3 = \beta \end{aligned} \tag{28}$$

The in-plane displacements of all the three elements at the crack node are equal and as a result, the mid-plane displacements of elements 1, 2 and 3 are related as:

$$\begin{aligned} u_2' &= u_1' - z_2\alpha \text{ and } v_2' = v_1' - z_2\beta \\ u_3' &= u_1' - z_3\alpha \text{ and } v_3' = v_1' - z_3\beta \end{aligned} \tag{29}$$

where u_1' is the mid- plane displacement of element 1. Equations (27),(28) and (29) relating the nodal displacements and rotations of elements 1,2 and 3 at the delamination crack tip, are multipoint constraint equations used in the finite element formulation to satisfy the compatibility of displacements and rotations.

Mid-plane strains between the element 2 and 3 are related as [24]

$$\{\varepsilon'\}_i = \{\varepsilon'\}_1 + z_i\{\kappa\} \quad (i = 2, 3) \tag{30}$$

where $\{k\}$ is the curvature vector being identical at the crack tip for element 2 and 3. This equation can be considered as a special case for element 1, when z_1 is equal to zero.

The in-plane stress resultants, $\{N\}$ and the moment resultants $\{M\}$ of element 2 and 3 can be expressed as [24]

$$\{N\}_i = [A]_i\{\varepsilon'\}_1 + (z_i[A]_i + [B]_i)\{\kappa\} \quad (i = 2, 3) \tag{31}$$

$$\{M\}_i = [B]_i\{\varepsilon'\}_1 + (z_i[B]_i + [D]_i)\{\kappa\} \quad (i = 2, 3) \tag{32}$$

where $[A], [B]$ and $[D]$ are extension, bending-extension coupling and bending stiffness coefficients of the composite laminate respectively and as follows[24]:

$$[A]_i = \int_{-\frac{h}{2}+z_i}^{\frac{h}{2}+z_i} [\overline{Q}]\, dz\,,\ [B]_i = \int_{-\frac{h}{2}+z_i}^{\frac{h}{2}+z_i} [\overline{Q}](z-z_i)\, dz\,,\ [D]_i = \int_{-\frac{h}{2}+z_i}^{\frac{h}{2}+z_i} [\overline{Q}](z-z_i)^2\, dz \tag{33}$$

Solution procedure

The global stiffness matrix ([K]) and load vector ([P]) are obtained by assembling the element stiffness matrices ([K_e]) and element load vectors([P_e]),respectively and then the following boundary conditions of the cantilever stiffened shell are imposed.

At x=0, u= v= w= α= β= 0 (34)

The solution to the following equilibrium equation is done employing Gauss elimination technique to obtain the global displacement vector $\{d\}$.

$$[K]\{d\} = \{P\} \tag{35}$$

The elemental displacement vectors are obtained from the global displacement vector thereafter the strains are evaluated at Gauss points using the equation(4). The force and moment resultants are calculated at these Gauss points by equations (7), (31) and(32).Then the values at the Gauss points are extrapolated to all the nodes of the shell. The calculation of in-plane stresses also follows the same procedure.

3. Results and Discussion

The mesh convergence study of a cantilever stiffened cylindrical shell with angle-ply and cross-ply laminates are illustrated in Table-1 considering the mesh size of 4×4, 6×6, 8×8 and 10×10 wherein it is observed that the percentage difference of non-dimensional center deflection in between 8×8 and 10×10 mesh size is less than unity, thus mesh size of 8×8 is used for the entire analysis for computational efficiency. For the entire analysis, the following material and geometric properties of graphite-epoxy composite stiffened cylindrical shell are employed:

E_1=138.0 GPa, E_2 =8.96 GPa, G_{12} = G_{13}= 7.1 GPa, G_{23} = 2.84 GPa, ν_{12} = 0.3, L/b = 1, b/h = 100, b/R_y = 0.5, $b_{st} = h$, $d_{st} = 2h$

The delamination is always considered through the complete width of the shell. Unless and otherwise stated, the number of layers and stacking sequence of the stiffeners are always same as that of the shell. The stiffeners are always placed along the span of the shell. The bending stiff ($[0_2/\pm 30]_s$) composite laminate is considered for the entire analysis. The in-plane stresses (σ_x, σ_y and τ_{xy}) are always evaluated at the top surface of the delaminated stiffened panel. Before continuing with parametric studies, the accuracy of the present finite element formulation is verified with the results available in the open literature [9, 12, 16,19, 25, 26]. The accuracy of the present formulation with respect to composite stiffened plate is shown in Table 2 wherein the discrepancies of the results with Kolli and Chandrashekhar [9] could be due to the fact that they used the mesh size of 4×4. The deflection, force and moment resultants of an orthotropic cylindrical shell are verified with Asadi et al.[25] and shown in Table 3, while the validity of in-plane stresses of a simply supported composite plate with Librescu and Khdeir [26] are displayed in Table 4. Due to non-availability of the static results of the pretwisted and delaminated shell, the free vibration results of the composite twisted plate and delaminated beam has been considered by incorporating the consistent mass matrix of the plate in the code. The simulated results of the pretwisted composite plates are shown in Table 5 while the frequency of a delaminated cantilever beam with varying the relative position of delamination is illustrated in Figure 3.

Table 1. Convergence study for non-dimensional transverse deflection ($\overline{w} = 10^3 wE_2h^3/(pL^4)$) of eight layered symmetric cross ply and angle ply stiffened cantilever cylindrical shell subjected to uniformly distributed load. ($L/b = 1, b/h = 100$, $b/R_y = 0.5$, $b_{st} = 2h$ and $d_{st} = 4h$, $n_x = n_y = 1$, eccentrically bottom stiffeners)

Stacking sequence	(4×4) Mesh	(6×6) Mesh	(8×8) Mesh	(10×10) Mesh
$[45/-45/45/-45]_s$	3.8332	3.9318	3.9775	4.0031
$[0/90/0/90]_s$	2.6974	2.7123	2.7153	2.7168

Table 2. Central deflection (mm) of a simply-supported cross ply[$0^0/90^0/90^0/0^0$] stiffened plate: L=254 mm, b=508mm, h=12.7 mm, b_x=6.35 mm, d_x=25.4mm, E_x=144.8GPa, E_y=9.65GPa, ν_{xy}=0.3, $G_{xy}=G_{xz}$=4.14 GPa, G_{yz}=3.45 GPa.

Number of x-stiffener	Uniform load P=0.6895N mm^{-2}			Concentrated load P=4.448kN	
	Kolli and Chandrashekhara[9]	Li and Xiaohui [12]	Present FEM	Kolli and Chandrashekhara[9])	Present FEM
0(un-stiffened)	1.9296	1.9395	1.9260	0.5136	0.5049
1	1.0396	1.1047	1.1018	0.2809	0.2923
2	1.5964	-	1.5939	0.4892	0.4850
3	0.9413	0.9407	0.9530	0.2725	0.2864

Table 3. Dimensionless central displacements and moments and force resultants of [$90^0/0^0$] orthotropic cylindrical shells subjected to uniformly distributed load. L/b = 1, Shear correction factor= 5/6, E_1/E_2 = 25, G_{12}/E_2 = 0.5, G_{23}/E_2 = 0.2, $G_{13} = G_{12}$, ν_{12} = 0.25. $\overline{w} = 10^3 E_y h^3 w/qL^4$, $\overline{M}_i = 10^3 M_i/qL^3$, $\overline{N}_i = 10^3 N_i/qL^2, i = x, y$.

Theory	L/h	L/R_y	$\overline{w}$	$\overline{M}_x$	$\overline{M}_y$	$\overline{N}_x$	$\overline{N}_y$
FSDT[25]			11.636	52.822	28.740	1083.4	996.77
3-D[25]	20	0.5	11.612	53.689	29.643	1084.7	990.78
Present			11.367	52.623	29.303	1077.2	1006.8

Table 4. Dimensionless central displacements and stresses of simple supported composite [0/90/0] plate: L/b = 1, E_1=19.2×10^6 psi, E_2 = 1.56×10^6 psi, $G_{12} = G_{13}$ = 0.82×10^6 psi, G_{23}= 0.523×10^6 psi, ν_{12}=0.24, $\overline{w} = w\left(0, \frac{b}{2}\right)\frac{10^2 E_2 h^3}{p_0 b^4}, \overline{\sigma}_{11} = \sigma_{11}\left(0, \frac{b}{2}, \frac{h}{2}\right)\frac{10h^2}{p_0 b^2}, \overline{\sigma}_{22} = \sigma_{22}\left(0, \frac{b}{2}, \frac{h}{6}\right)\frac{10h^2}{p_0 b^2}$

b/h		Librescu and Khdeir [26]	Present FEM
2	$\overline{w}$	7.058	7.0881
	$\overline{\sigma}_{11}$	5.020	5.0581
	$\overline{\sigma}_{22}$	5.984	6.0314
5	$\overline{w}$	2.273	2.2611
	$\overline{\sigma}_{11}$	6.512	6.5637
	$\overline{\sigma}_{22}$	3.303	3.3272
10	$\overline{w}$	1.484	1.4687

	$\overline{\sigma}_{11}$	7.036	7.0922
	$\overline{\sigma}_{22}$	2.342	2.3578
	$\overline{w}$	1.277	1.2599
20	$\overline{\sigma}_{11}$	7.196	7.2531
	$\overline{\sigma}_{22}$	2.042	2.0534

Table 5. Non-dimensional fundamental frequencies($\varpi = \omega_n L^2 \sqrt{\rho / E_{11} h^2}$) of three layer[$\theta,-\theta,\theta$] graphite-epoxy twisted plates. *L/b*=1,*b/h*=20,Twist angle(ϕ)=30^0 ,E_{11}=138.70 GPa, E_{22}=8.96 GPa, G_{12}=7.1 Gpa, ν_{12}=0.3

θ (Deg.)	Qatu and Leissa [19]	Present FEM
0	0.9553	0.9431
15	0.8759	0.8629
30	0.6923	0.6812
45	0.4831	0.4752
60	0.3283	0.3245
75	0.2582	0.2572
90	0.2434	0.2431

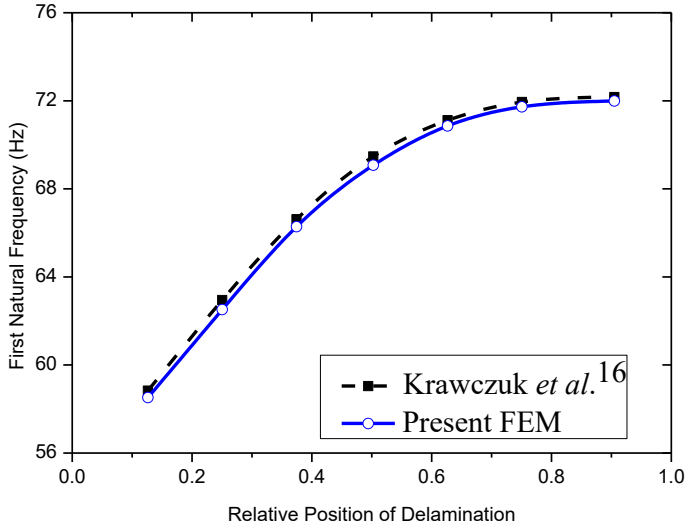

Figure 3. The influence of relative position of delamination on the first natural frequency of composite cantilever beam. Matrix (epoxy resin) [$E = 3.43$ GPa, $\nu = 0.35$, $\rho = 1250$ kg/m³] and fibres (graphite) [$E = 275.6$ GPa, $\nu = 0.2$, $\rho = 1900$ kg/m³, $L = 600$ mm, $b = 50$ mm, $h = 25$ mm, volume fraction of fiber=0.3, $a = 37.5$ mm]

Anusandhanvallari
Vol 2023, No.1
June 2023
ISSN 2229-3388

Effect of number of stiffeners:

A comparative study of both unstiffened and stiffened cylindrical shell are presented in Figure 4, considering mid-plane delamination of 50% at the mid-span. The non-dimensional bending parameters such as deflection, and in-plane stresses of delaminated cantilever composite shells are illustrated and the non-dimensional force and moment resultants at the mid-span are presented in Table 6. Eccentric top stiffeners along x-direction are considered within the shell. The variation of the bending parameters along the centerline of the shell in the span wise direction is shown. As expected, the non-dimensional deflection(NDD) of the shell decreases due to the addition of stiffener. Moreover, increasing the number of stiffeners also reduces the deflection because of the increase in elastic stiffness of the panel. The maximum deflection is found at the free end of the stiffened shell as normally seen in a cantilever shell. It is evident that maximum value of $\overline{\sigma}_x$ is found at the fixed end and gradually it diminishes till the mid-span again increases up to free end, where its value is zero. The nature of $\overline{\sigma}_x$ is found tensile near the fixed end and thereafter it gradually becomes compressive. The increase in the number of stiffeners reduces the peak value of $\overline{\sigma}_x$ wherein the maximum value of $\overline{\sigma}_x$ is obtained corresponding to n_x= 0 followed by n_x= 1 and 3. The same trend is also observed for $\overline{\sigma}_y$ wherein its value is found zero near the fixed end and maximum at the free end. The variation of $\overline{\tau}_{xy}$ is observed to vary from tensile nature to compressive from fixed end to free end. The addition of a single stiffener increases the value of shear stress while at n_x=3 the tensile value of shear stress reduces and increases the compressive value than that of the un-stiffened shell near the fixed and free end, respectively. From the Table 6, it is evident that addition of stiffeners reduced the value of both $\overline{M}_x$ and $\overline{M}_{xy}$ while increases the value of $\overline{N}_y$.

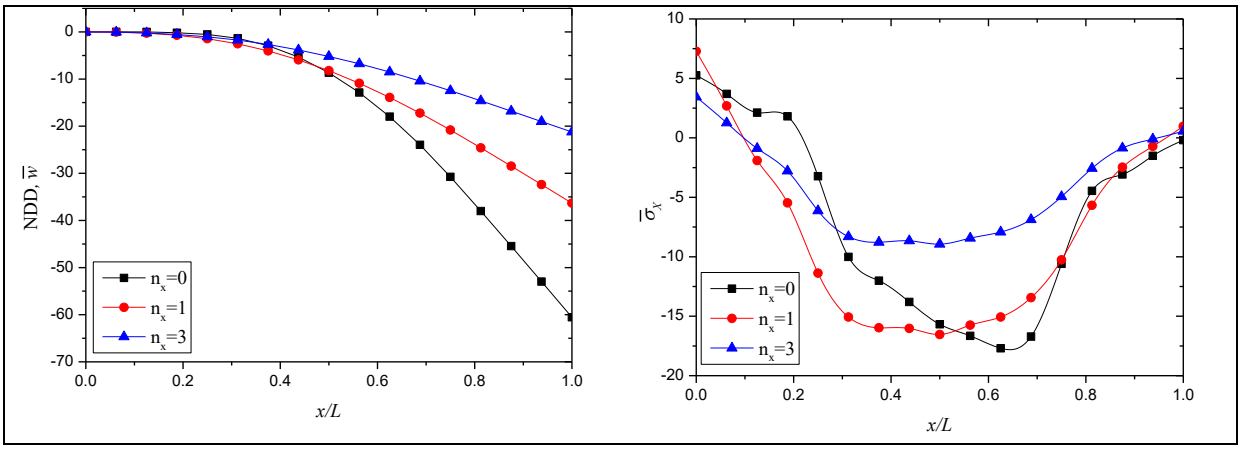

Anusandhanvallari
Vol 2023, No.1
June 2023
ISSN 2229-3388

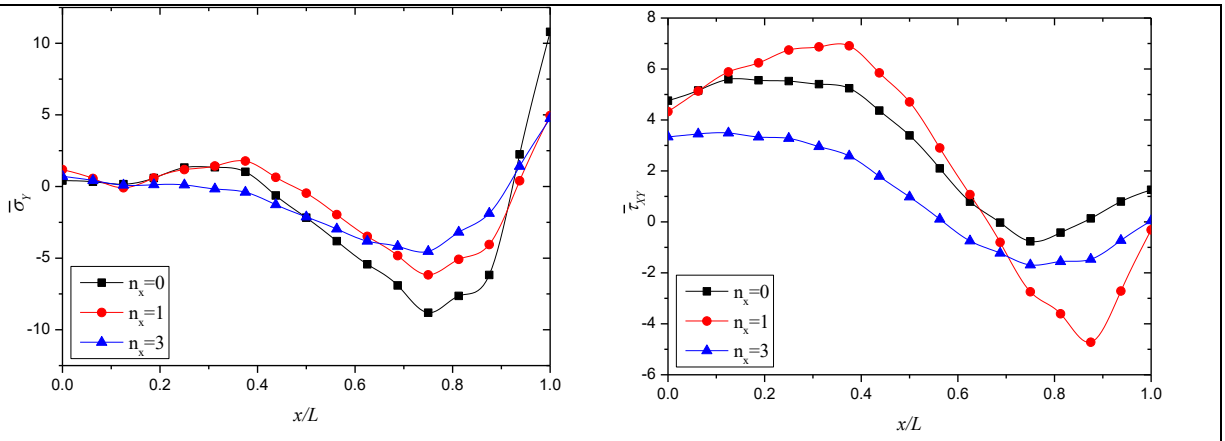

Figure 4. Effects of number of stiffeners on non-dimensional deflection and in-plane stresses of bending stiff composite delaminated stiffened cylindrical shell with pretwisted subjected to uniformly distributed load. a/L=0.5, h'/h =d/L= 0.5, Φ =15^0

Table 6. Effects of number of stiffeners on non-dimensional deflection and stress resultants at the centre of the bending stiff composite delaminated stiffened cylindrical shell with pretwisted subjected to uniformly distributed load. a/L=0.5, h'/h =d/L= 0.5, Φ =15^0

n_x	$\overline{w}$	$\overline{N}_x$	$\overline{N}_y$	$\overline{N}_{xy}$	$\overline{M}_x$	$\overline{M}_y$	$\overline{M}_{xy}$
0	-8.6547	3737.735	-1050.2247	2062.927	82.7724	1.3772	-1.7962
1	-8.2190	-12034.536	-2736.3521	4885.869	36.4048	-5.9824	-0.8235
3	-5.1982	-6558.474	-3710.3601	648.5799	19.2763	-2.9785	-0.4746

Effects of twist angle:

The non-dimensional deflection and in-plane stresses with the variation of initial twist angles of the delaminated stiffened panel with one x-directional stiffener are illustrated in Figure 5. and the non-dimensional force and moment resultants at the center of the delaminated stiffened shell are furnished in Table 7. It evident that deflection at the free end of the stiffened shell increases rapidly as twist angles increase, this may be due to the fact that increase in twist angle reduces the elastic stiffness. That is, the deflection of the untwisted stiffened shell is very less as compared to that of the twisted cases. In untwisted stiffened shell the nature of $\overline{\sigma}_x$ is found tensile while increasing in twist angle makes it compressive. The value of $\overline{\sigma}_x$,which is compressive in nature also increases as twist angle increases but the finally at x=L the value of $\overline{\sigma}_x$ is found zero in all the cases. However, the nature of the stress $\overline{\sigma}_y$ is found fluctuating in twisted cases. The magnitude of $\overline{\sigma}_y$ is found maximum at the free end wherein tensile and compressive stresses ($\overline{\sigma}_y$) are induced in twisted and in untwisted stiffened shell, respectively. The variation of $\overline{\tau}_{xy}$ in untwisted case is found insignificant compared to twisted cases. It may be noted that the magnitude of stress and moment resultants at the mid-span increases with increase in twist angle except $\overline{M}_y$ wherein the value decreases with increase in twist angle but the sudden changes in $\overline{N}_{xy}$ and $\overline{M}_{xy}$ is remarkable.

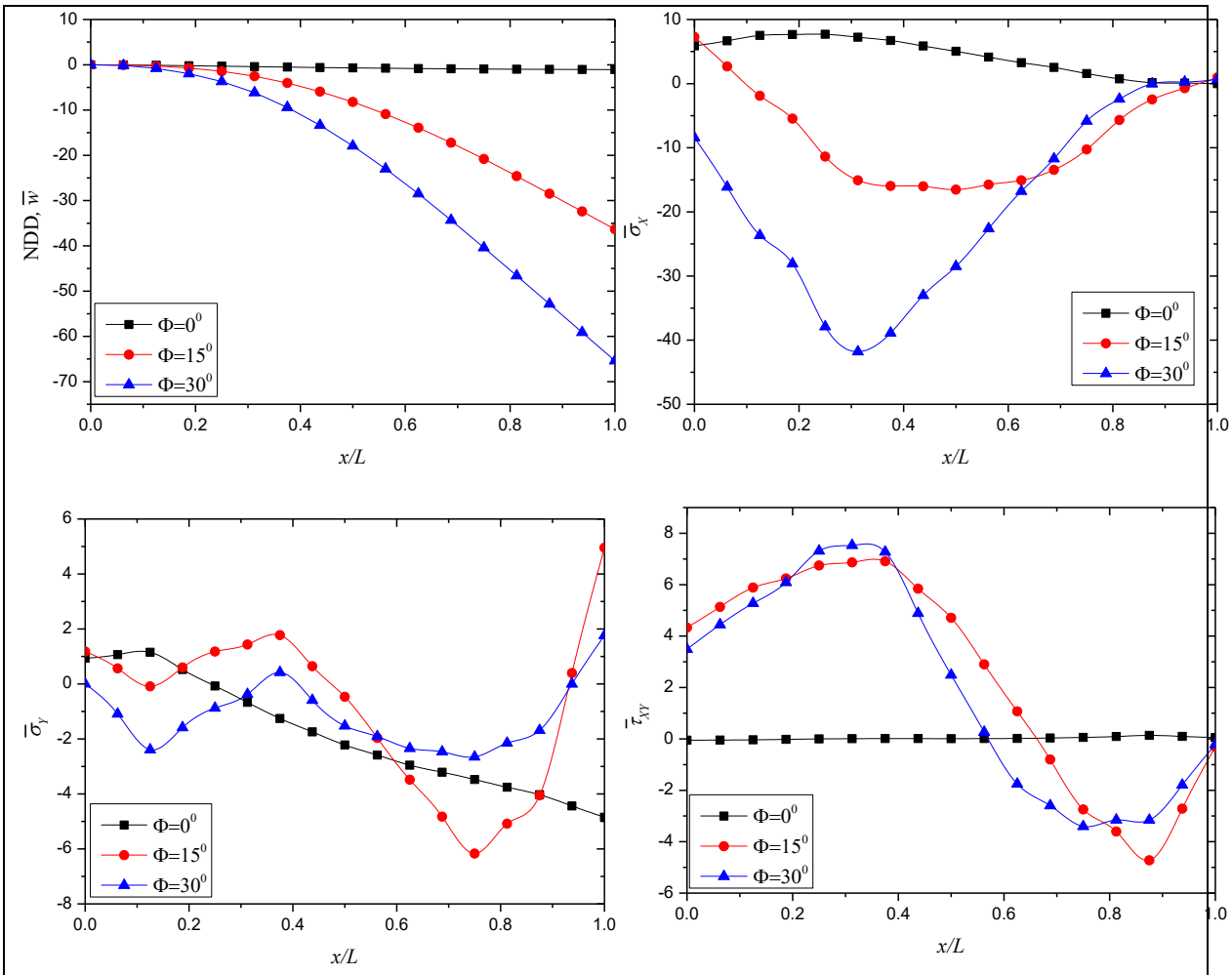

Figure 5. Effects of twist angle on non-dimensional deflection, moment resultants and in-plane stresses of bending stiff composite delaminated stiffened cylindrical shell subjected to uniformly distributed load. a/L=0.5, h'/h =d/L= 0.5, Φ =15^0, n_x=1.

Table 7. Effects of initial twist on the non-dimensional deflection, force and moment resultants and in-plane stresses at the centre of the bending stiff composite delaminated stiffened cylindrical shell subjected to uniformly distributed load , a/L=0.5, h'/h =d/L= 0.5, n_x=1 .

Twist Angle (Φ)	$\overline{w}$	$\overline{N}_x$	$\overline{N}_y$	$\overline{N}_{xy}$	$\overline{M}_x$	$\overline{M}_y$	$\overline{M}_{xy}$
0^0	-0.6906	6256.807	-2189.51	11.94143	5.5265	10.6343	-0.0087
15^0	-8.2190	-12034.5	-2736.35	4885.87	36.4048	-5.9824	-0.8235
30^0	-17.9150	-23049.5	-3149.11	2362.066	49.0905	-4.2799	-0.6156

Effect of delamination across the thickness:

The normalized deflection, moment resultants and in-plane stress values at the center of the bending stiff twisted composite stiffened shell is presented in Table 8 by varying the position of delamination across the thickness of

the shell wherein 50% delamination at the mid-span is considered in all the cases and a single eccentric top stiffener is placed at the center line along the longitudinal direction. It is evident that non-dimensional deflection($\overline{w}$) significantly increases as the delamination moves towards mid-plane (h'/h=0.5), wherein it found the maximum and thereafter decreases till the bottom ply. The values of both $\overline{M}_x$ and $\overline{\sigma}_x$ also decreases till h'/h=0.625 and again increases as delamination shifts towards the bottom ply, while the value of M_{xy} decreases till the mid-ply and then again increases. The stress $\overline{\sigma}_y$ decreases from top ply to mid-plane and thereafter increases. The nature of variation of $\overline{\tau}_{xy}$ is similar to that of $\overline{w}$. Due to the presence of x- directional stiffener the values of both $\overline{M}_x$ and $\overline{\sigma}_x$ is found greater than that of $\overline{M}_y$ and $\overline{\sigma}_y$,respectively.

Table 8. Effects of delamination across the thickness of the bending stiff pretwisted composite stiffened cylindrical shell subjected to uniformly distributed load. The parameters are evaluated at x/L=0.5 , a/L=0.5, d/L= 0.5, $\Phi=15^0$, n_x=1.

h'/h	$\overline{w}$	$\overline{M}_x$	$\overline{M}_y$	$\overline{M}_{xy}$	$\overline{\sigma}_x$	$\overline{\sigma}_y$	$\overline{\tau}_{xy}$
0.000	-6.8667	74.5317	2.7173	-10.3862	-10.7704	-3.8099	1.4640
0.125	-7.1866	54.4824	0.4639	-9.7858	-12.8571	-3.1101	2.1310
0.25	-7.5583	34.0041	-1.5359	-9.6883	-14.9578	-2.2492	3.0302
0.375	-7.7512	41.3187	-0.2847	-7.8825	-14.9443	-1.5541	3.7303
0.500	-8.2190	36.4048	-5.9824	-0.8235	-16.5337	-0.4673	4.7080
0.625	-7.9078	33.9129	-5.8012	-1.4270	-16.6436	-1.7772	3.7838
0.750	-7.5454	36.7376	-5.2987	-5.4070	-15.6138	-2.3029	3.2546
0.875	-7.1895	54.5426	-1.6357	-8.0138	-13.1231	-3.0983	2.2411

Effect of delamination along the span

Figure 6 shows the variation of normalized bending parameters of the bending stiff twisted($\Phi=15^0$) composite stiffened shell with varying the position of delamination along the span. A mid-plane delamination of 50% is considered at three different positions(d/L=0.25, 0.5 and 0.75) and the variation of non-dimensional parameters are shown along the centre line in the longitudinal direction. It may note that at d/L=0.25 the non-dimensional deflection is found maximum while minimum at d/L= 0.75. That is, deflection goes on reducing as delamination shifts from fixed end to free end while it is observed that the value of $\overline{M}_x$ rapidly drops particularly at the zone of delamination and again increases and finally attains zero. The maximum value of $\overline{M}_x$ is attained before the delamination zone in case of d/L=0.5 and 0.75 while incase if d/L=0.25 it happens after the end of delamination zone. It is evident that the maximum value of $\overline{M}_y$ is found at the free end and zero at x=0 in all the three cases wherein the value of $\overline{M}_y$ suddenly decreases at delamination zone and after that, it again increases. In all the three cases, the nature of $\overline{\sigma}_x$ is found tensile at the fixed end and gradually the value turns to compressive and finally zero at the free end. The increase of compressive stress($\overline{\sigma}_x$) in the zone of delamination is depicted in all the cases. The maximum value of $\overline{\sigma}_y$ is found at the free end whereas at the fixed end the value is almost zero. The variation of $\overline{\tau}_{xy}$ along the center line in the longitudinal direction at the top surface is observed as sinusoidal while the peak value of $\overline{\tau}_{xy}$ is obtained maximum corresponding to d/L=0.25 in tension but corresponding d/L=0.75 it is maximum in compression.

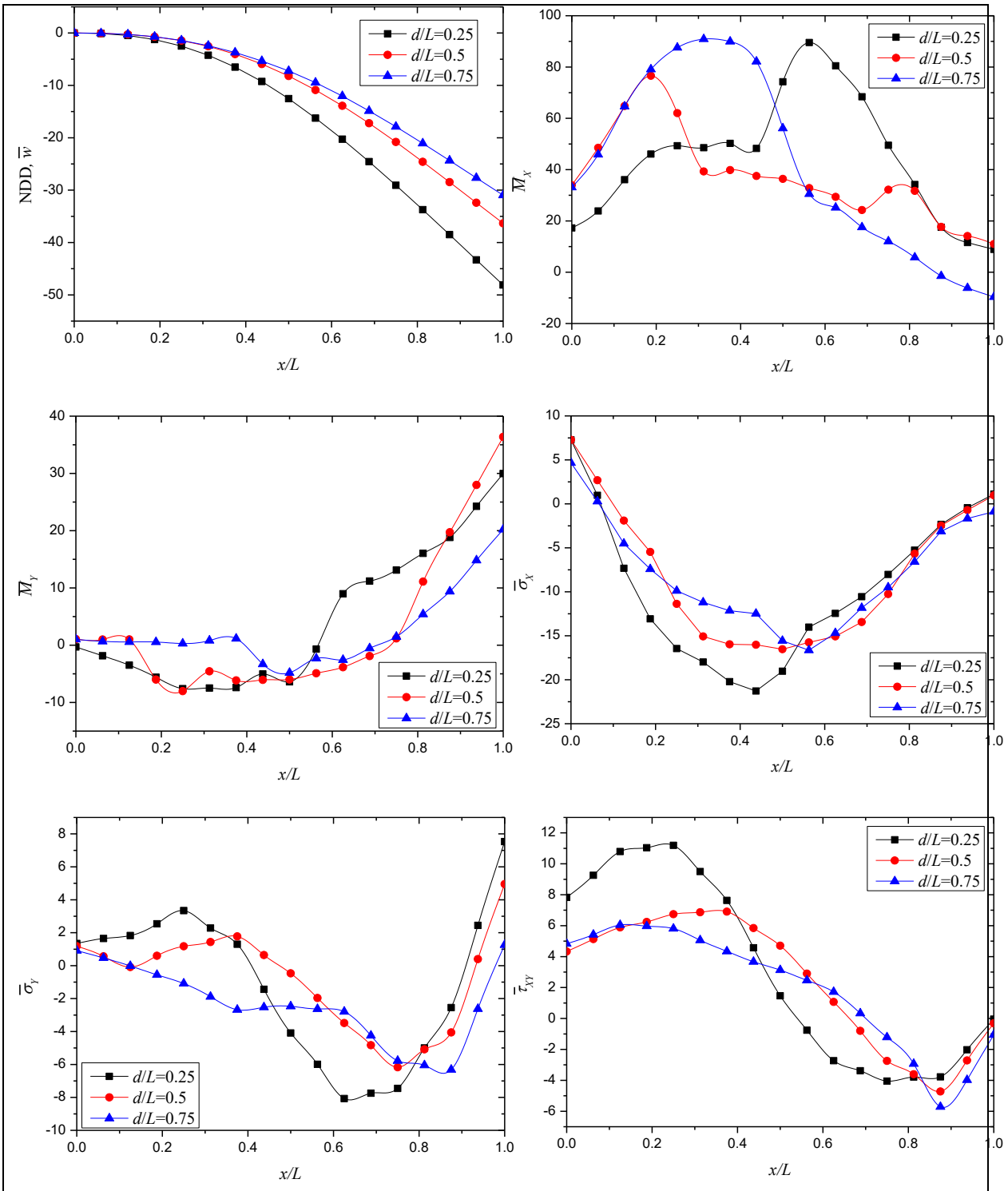

Figure 6. Effects of variation of delamination along the span on non-dimensional deflection, moment resultants and in-plane stresses of the bending stiff composite delaminated stiffened cylindrical shell with pretwisted subjected to uniformly distributed load. Pd $h'/h = d/L = 0.5$, $\Phi = 15^0$, $n_x = 1$.

Anusandhanvallari
Vol 2023, No.1
June 2023
ISSN 2229-3388

Effect of percentage of delamination

The influence of percentage of delamination($(a/L)\times 100$) on the static response of the pretwisted(Φ =15^0) stiffened shell is illustrated in Figure 7, wherein the non-dimensional parameters are evaluated corresponding to delamination 0 %, 25 %, 50 % and 75 % at the mid-plane (h'/h= d/L=0.5), respectively. Being a cantilever stiffened shell, large deflection is observed at the free end while minimum and maximum deflections are observed corresponding to 0% and 75% of delamination. Delamination in the structure reduces the stiffness and strength thereby increases the deflection. In the intact stiffened shell(Pd=0), value of $\overline{M}_x$ increases from the fixed end to the ultimate value and thereafter reduces approximately to zero at the free end while in case of delaminated cases, $\overline{M}_x$ is found to increase in the same pattern of intact case initially but decrease rapidly particularly at the zone of delamination and thereafter again increases and follows the same trend of intact stiffened shell. The characteristics also observed for inplane stress ($\overline{\sigma}_x$), wherein maximum compressive stress is obtained at the mid span in all the cases. It is evident that maximum compressive stress ($\overline{\sigma}_x$)is obtained corresponding to 75% delamination and minimum in the intact stiffened shell. The variation of $\overline{M}_y$ shows that maximum value is attained at the free end while approximately zero at the fixed end. The variation of $\overline{M}_y$ and $\overline{\sigma}_y$ is similar to each other wherein increase in the percentage of delamination increases both the values at the free end. The values of $\overline{\sigma}_y$ and $\overline{\tau}_{xy}$ are very small as compared to the value of $\overline{\sigma}_x$. It is further observed that increase in delamination area increases the value of shear stress $\overline{\tau}_{xy}$ except in 25 % delamination case and however the nature of the in-plane stress changes i.e. tensile to compressive from fixed end to free end.

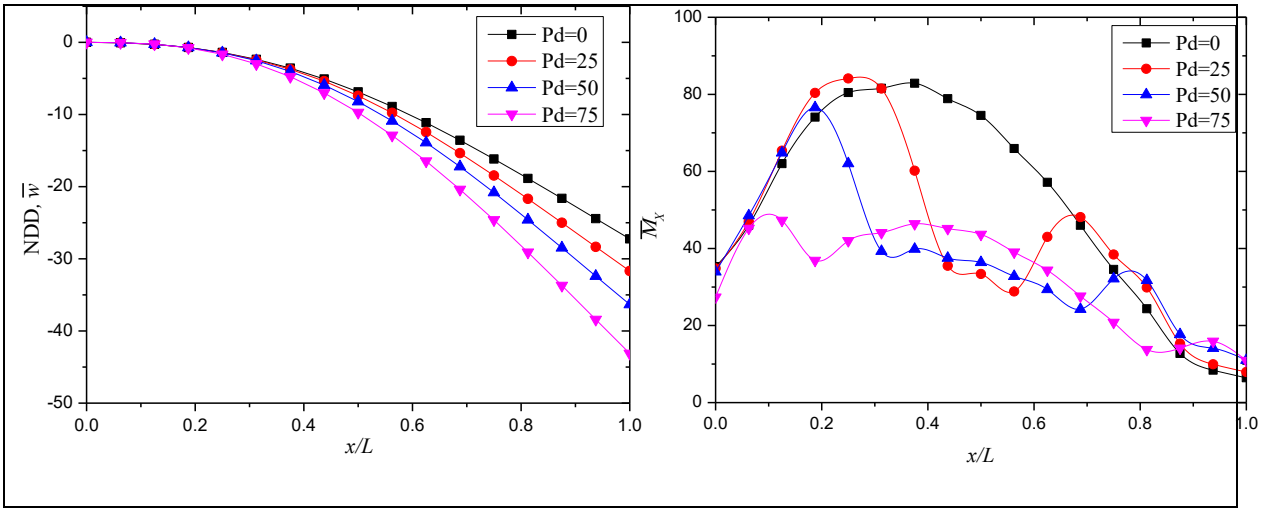

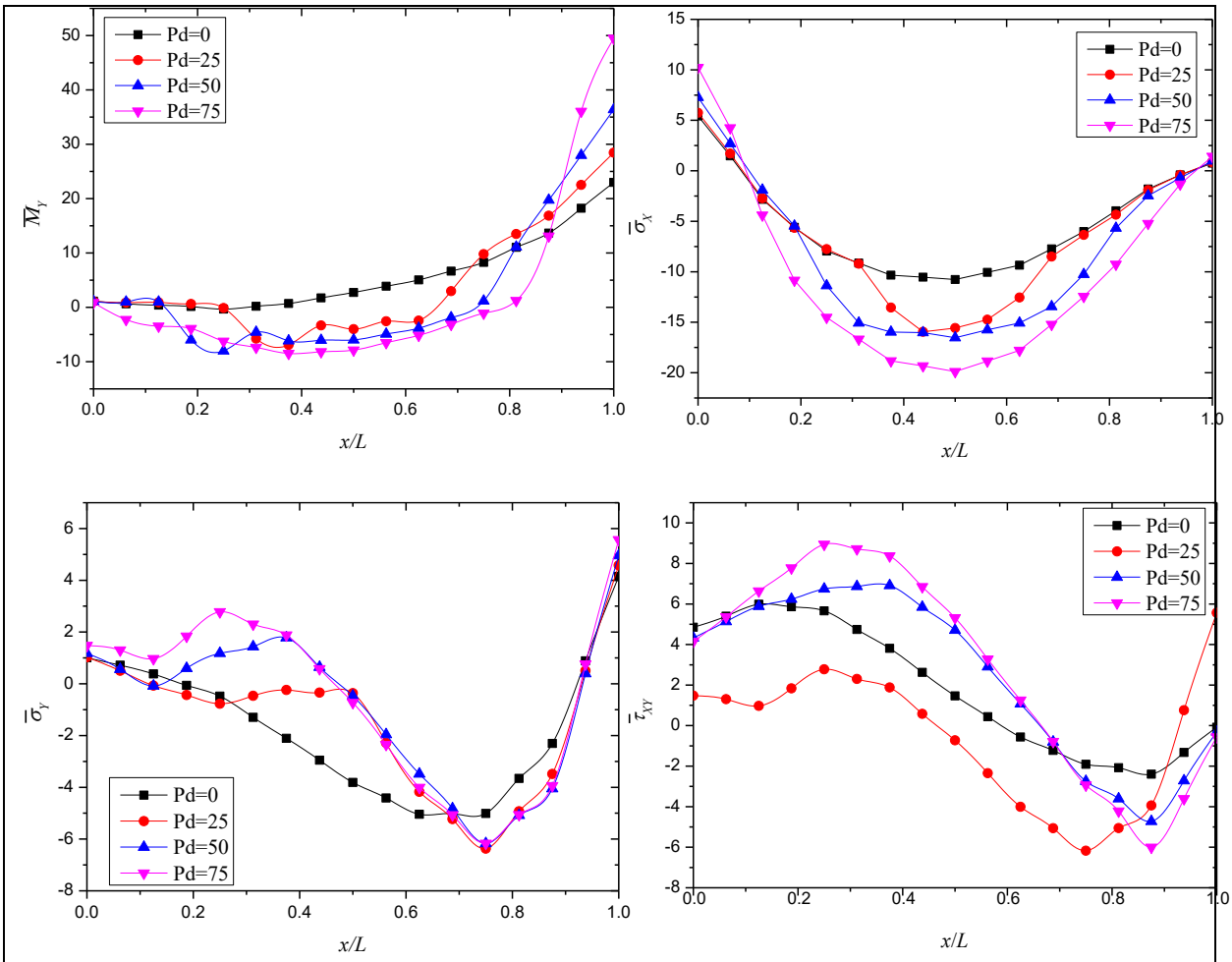

Figure 7. Effects of percentage of delamination on non-dimensional deflection, moment resultants and in-plane stresses of the bending stiff composite delaminated stiffened cylindrical shell with pretwisted subjected to uniformly distributed load. $h'/h = d/L = 0.5$, $\Phi = 15^0$, $n_x = 1$
Note: Pd-Percentage of delamination

Effect of eccentricity of stiffener

It is evident from the literature that eccentricity of the stiffener has a remarkable effect on the natural frequency of the panel, thus its effect on bending characteristics of the delaminated twisted panel is examined and shown in Figure 8. The non-dimensional transverse deflection is found the maximum in the concentric stiffener whereas minimum in eccentric top stiffener. Moreover, there is a marginal difference between the two deflection curves meant for the eccentric top and eccentric bottom stiffener towards the free end. Eccentric top stiffener renders maximum stiffness to the structure thereby less deflection because of the high value of the moment of inertia due to positive eccentricity. $\overline{M}_x$ is found maximum in the concentric stiffened shell at the mid-span while no significant difference is observed in the case of eccentric top and bottom stiffeners. $\overline{M}_y$ is found to be maximum in eccentric stiffeners at the free end than that of the concentric stiffeners. In the above discussion, it

justifies the preference of the eccentric stiffeners, especially the eccentric top. It is quite interesting to observe that eccentric bottom stiffeners induce tensile stress ($\bar{\sigma}_x$) while the eccentric top and concentric stiffeners compressive stress($\bar{\sigma}_x$). The nature of the stress $\bar{\sigma}_x$ may be different but the magnitude of the stress $\bar{\sigma}_x$ obtained is found maximum on eccentric top stiffeners followed by the eccentric bottom and concentric. The magnitude of $\bar{\sigma}_y$ is observed almost zero till the mid-span from the fixed end thereafter it becomes compressive and then tensile at the free end. The maximum tensile value of $\bar{\sigma}_y$ is obtained in eccentric bottom stiffener followed by concentric and eccentric top while in compressive nature, the maximum magnitude is found in eccentric top followed by the eccentric bottom and concentric. However, the variation of $\bar{\sigma}_y$ with respect to the three types of stiffeners are found almost marginal. The magnitude of $\bar{\tau}_{xy}$ is found the maximum in eccentric top stiffeners but the nature of the shear stress changes from tensile to compressive. The magnitude of $\bar{\tau}_{xy}$ is found negligible as compared to $\bar{\sigma}_x$ and $\bar{\sigma}_y$.

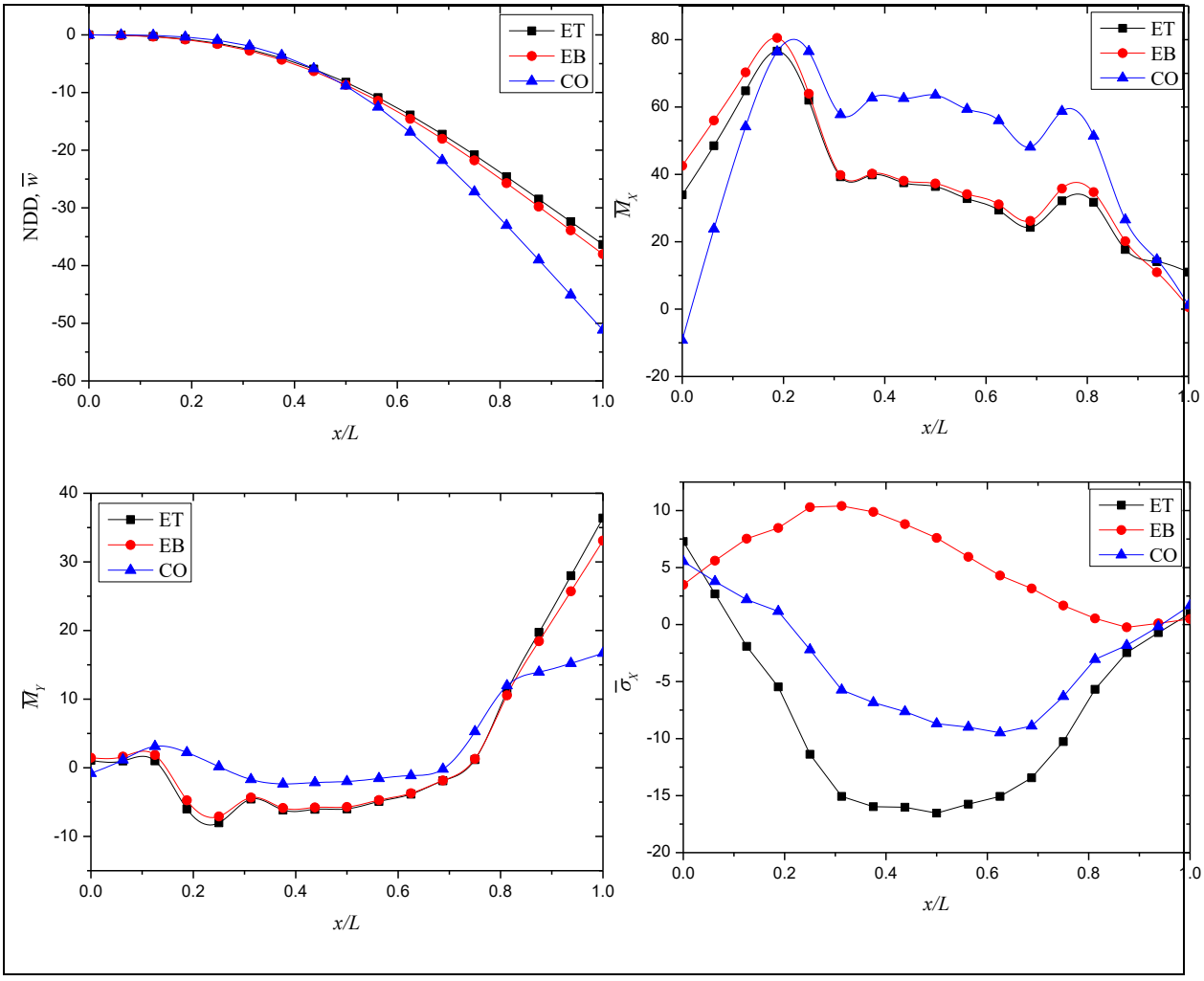

Anusandhanvallari
Vol 2023, No.1
June 2023
ISSN 2229-3388

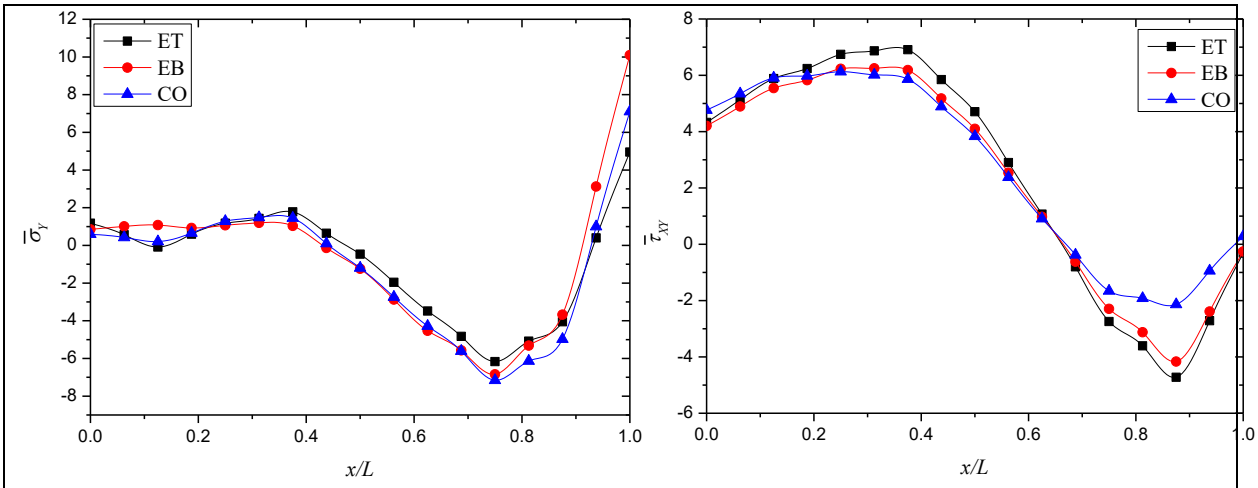

Figure 8. Effects of eccentricity of stiffener on non-dimensional deflection, moment resultants and in-plane stresses of the bending stiff composite delaminated stiffened cylindrical shell with pretwisted subjected to uniformly distributed load. $h'/h = d/L = 0.5$, $\Phi = 15^0$, $n_x = 1$
Note: ET-Eccentric top, EB-Eccentric bottom, CO-Concentric

Effect of stiffener depth to shell thickness ratio (d_{st}/h)

Figure 9 shows the values of bending parameters of a delaminated twisted stiffened cylindrical shell with varying the thickness of the stiffener. This study, however, is useful in deciding the depth of stiffener for a particular thickness of the shell. The value of $\overline{w}$ decreases with increasing value of d_{st}/h and is clearly observed towards the free end. It is worth mentioning that the maximum value of vertical deflection is observed at d_{st}/h =1.0 while minimum at d_{st}/h =3.0. The maximum and minimum value of $\overline{M}_x$ is obtained corresponding to d_{st}/h=1.0 and 3.0, respectively, while the value suddenly decreases at the mid-span i.e. the zone of delamination. The moment resultant $\overline{M}_y$ is found to increase from fixed end to free end in all the cases while maximum value at the free end is obtained corresponding to d_{st}/h =3.0. Higher is the thickness of the stiffener higher is the value of $\overline{M}_y$ at free end but in contrast at mid-span higher value of thickness of stiffener reduces the value of $\overline{M}_y$. The variation of $\overline{\sigma}_x$ is shows that the stress is tensile near the fixed end and thereafter it becomes gradually compressive in nature wherein maximum compressive stress is obtained at the mid-span in almost all the cases except at d_{st}/h =3.0. It is observed that increases in the thickness of the stiffener particularly at d_{st}/h =3.0 the stress at fixed end becomes compressive in nature. Insignificant variation of $\overline{\sigma}_y$ and $\overline{\tau}_{xy}$ is observed with variation in thickness of the stiffener. However, increase in d_{st}/h reduces the value of $\overline{\sigma}_y$ at the free end.

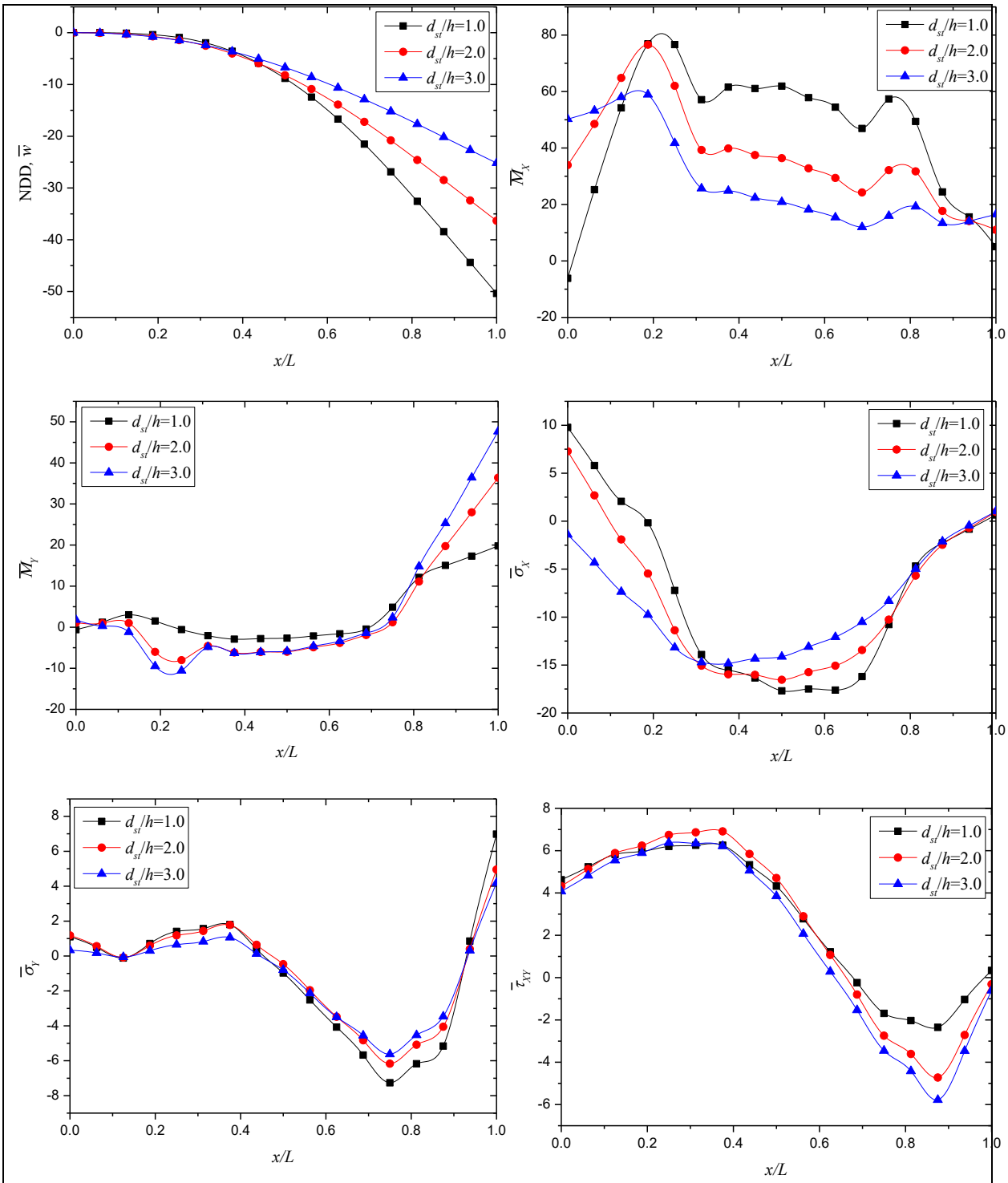

Figure 9. Effects of stiffener depth to shell thickness ratio on non-dimensional deflection, moment resultants and in-plane stresses of the bending stiff composite delaminated stiffened cylindrical shell with pretwisted subjected to uniformly distributed load. $h'/h = d/L = 0.5$, $\Phi = 15^0$, $n_x = 1$.

4. Conclusion

Bending characteristics of twisted composite stiffened shells with delamination subjected transverse load is studied by employing finite element method. The mathematical model of both shell and stiffeners have been established separately. Multipoint constraint algorithm is incorporated in the finite element code to model delamination. A variety of numerical examples are presented to perform parametric study. The captivating conclusions made from the parametric studies are listed below:

1. Addition of stiffeners reduces the value of $\overline{w}$, $\overline{\sigma}_x$ and $\overline{\sigma}_y$ to a great extent because of increase in elastic stiffness of the panel.

2.Twist angle has a prominent effect on the performance of the stiffened shell, wherein increase in its value increases the value of $\overline{w}$ due to reduction in elastic stiffness. Twist angle induces compressive stress $\overline{\sigma}_x$ in the shell. However, its effect is found insignificant on $\overline{\tau}_{xy}$.

3. As delamination along the span is concerned, the transverse deflection is found maximum when delamination is located near the fixed end and across the thickness, deflection increases as the delamination moves towards the mid-plane of the stiffened shell laminate. Increase in percentage of delamination also increases the transverse deflection and in-plane stresses.

4. The eccentric stiffeners renders maximum stiffness than concentric thereby reduces the value of transverse deflection. Eccentricity of the stiffeners has remarkable effects on the nature of stresses, especially on $\overline{\sigma}_x$.

5. A higher drop in the transverse deflection of the stiffened shell is observed as thickness of the stiffener is increased.

References:

[1] Rossow MP, Ibrahimkhail AK. Constraint method analysis of stiffened plates. Comput. Struct. 1978;8(1):51-60.
[2] Venkatesh A, Rao KP. Analysis of laminated shells with laminated stiffeners using rectangular shell finite elements. Comput. Methods Appl. Mech. Eng. 1983;38(3):255-72.
[3] Venkatesh A, Rao KP. Analysis of laminated shells of revolution with laminated stiffeners using a doubly curved quadrilateral finite element. Comput. Struct.1985;20(4):669-82.
[4] Liao CL, Reddy JN. Analysis of anisotropic, stiffened composite laminates using a continuum-based shell element. Comput. Struct. 1990;34(6):805-15.
[5] Chattopadhyay B, Sinha PK, Mukhopadhyay M. Finite element analysis of blade-stiffened composite plates under transverse loads. J. Reinf. Plast. Compos. 1993;12(1):76-100.
[6] Goswami S, Mukhopadhyay M. Finite element analysis of laminated composite stiffened shell. J. Reinf. Plast. Compos. 1994;13(7):574-616.
[7] Mukherjee A, Menghani LC. Displacement and stress response of laminated beams and stiffened plates using a high-order element. Compos. Struct. 1994;28(1):93-111.
[8] Sinha GO, Mukhopadhyay MA. Static and dynamic analysis of stiffened shells–a review. InProc. Indian Natn. Sci. Acad. A 1995; 61:195-219.
[9] Kolli M, Chandrashekhara K. Finite element analysis of stiffened laminated plates under transverse loading. Compos. Sci. Technol. 1996;56(12):1355-61.
[10] Sadek EA, Tawfik SA. A finite element model for the analysis of stiffened laminated plates. Comput. Struct. 2000;75(4):369-83.

[11] Prusty BG. Linear static analysis of composite hat-stiffened laminated shells using finite elements. Finite Elem. Anal. Des. 2003;39(12):1125-38.
[12] Li L, Xiaohui R. Stiffened plate bending analysis in terms of refined triangular laminated plate element. Compos. Struct. 2010;92(12):2936-45.
[13] Das HS, Chakravorty D. Bending analysis of stiffened composite conoidal shell roofs through finite element application. J. Compos. Mater. 2010 ;45(5):525-542.
[14] Bhaskar K, Pydah A. An elasticity approach for simply-supported isotropic and orthotropic stiffened plates. Int. J. Mech. Sci. 2014;89:21-30.
[15] Shen MH, Grady JE. Free vibrations of delaminated beams. AIAA J. 1992;30(5):1361-70.
[16] Krawczuk M, Ostachowicz W, Zak A. Dynamics of cracked composite material structures. Comput. Mech. 1997;20(1):79-83.
[17] Karmakar A, Kishimoto K. Free Vibration Analysis of Delaminated Composite Pretwisted Rotating Shells─ A Finite Element Approach. JSME Int J., Ser. A. 2006;49(4):492-502.
[18] Bandyopadhyay T, Karmakar A. Bending characteristics of delaminated cross-ply composite shallow conical shells in hygrothermal environment. J. Reinf. Plast. Compos. 2015;34(20):1724-35.
[19] Qatu MS, Leissa AW. Vibration studies for laminated composite twisted cantilever plates. Int. J. Mech. Sci. 1991;33(11):927-40.
[20] Kuang JH, Hsu MH. The effect of fiber angle on the natural frequencies of orthotropic composite pre-twisted blades. Compos. Struct. 2002;58(4):457-68.
[21] Lee JJ, Yeom CH, Lee I. Vibration analysis of twisted cantilevered conical composite shells. J. Sound Vib. 2002;255(5):965-82.
[22] Kee YJ, Kim JH. Vibration characteristics of initially twisted rotating shell type composite blades. Compos. Struct. 2004;64(2):151-9.
[23] Thirupathi SR, Seshu P, Naganathan NG. A finite-element static analysis of smart turbine blades. Smart Mater. Struct. 1997;6(5):607.
[24] Gim CK. Plate finite element modeling of laminated plates. Comput. Struct. 1994;52(1):157-68.
[25] Asadi E, Wang W, Qatu MS. Static and vibration analyses of thick deep laminated cylindrical shells using 3D and various shear deformation theories. Compos. Struct. 2012;94(2):494-500.
[26] Librescu L, Khdeir AA. Analysis of symmetric cross-ply laminated elastic plates using a higher-order theory: Part I—Stress and displacement. Compos. Struct. 1988;9(3):189-213.